Taylor & Francis
Taylor & Francis Group

Combustion Science and Technology

ISSN: 0010-2202 (Print) 1563-521X (Online) Journal homepage: www.tandfonline.com/journals/gcst20

Importance of Energy and Molecular Transport on the Modeling of Explosion Limit and Explosion Behavior of Hydrogen-Oxygen Mixtures

Chunkan Yu , Liming Cai & Ulrich Maas

To cite this article: Chunkan Yu , Liming Cai & Ulrich Maas (17 Sep 2026): Importance of Energy and Molecular Transport on the Modeling of Explosion Limit and Explosion Behavior of Hydrogen-Oxygen Mixtures, Combustion Science and Technology, DOI: 10.1080/00102202.2026.2734842

To link to this article: https://doi.org/10.1080/00102202.2026.2734842

Published online: 17 Sep 2026.

COMBUSTION SCIENCE AND TECHNOLOGY
https://doi.org/10.1080/00102202.2026.2734842

Importance of Energy and Molecular Transport on the Modeling of Explosion Limit and Explosion Behavior of Hydrogen-Oxygen Mixtures

Chunkan Yu[a], Liming Cai[b], and Ulrich Maas[a]

[a]Institute of Technical Thermodynamics, Karlsruhe Institute of Technology, Karlsruhe, Germany; [b]School of Automotive Studies, Tongji University, Shanghai, China

ABSTRACT

Despite the classical developments and subsequent studies of individual transport mechanisms, many recent explosion-limit simulations still apply homogeneous formulations. Many recent study on explosion limits of reactive mixtures focuses on the usage of homogeneous models that neglect spatial transport processes. However, energy and molecular transport processes can show a profound influence on explosion behavior that cannot be captured under homogeneous assumptions. This motivates a systematic reassessment of the physical importance of energy and molecular transport within a unified spatially resolved framework. This work investigates the role of spatially resolved energy and molecular transport in explosion phenomena using a stoichiometric hydrogen-oxygen mixture as a reference system. Explosion limits and subsequent flame behavior are analyzed by solving one-dimensional governing equations incorporating detailed chemical kinetics, molecular diffusion, surface reactions and wall heat loss. Results show that the first and second explosion limits are predominantly chemically controlled and largely insensitive to thermal boundary conditions. In contrast, the third explosion limit is governed by the competition between heat release and wall heat loss, confirming its thermal nature. Wall heat transfer strongly alters the critical explosion temperature, indicating the decisive role of spatial temperature inhomogeneity. Thermal diffusion is negligible under the present conditions, whereas differential diffusion of radicals plays distinct roles: enhanced H diffusion significantly accelerates post-ignition flame propagation, while enhanced H_2O_2 diffusion suppresses explosion by weakening local chain-branching activity. These findings suggest that explosion limits and explosion behavior are intrinsically controlled by the coupling between chemical kinetics, energy transport and molecular diffusion. Accurate and physically consistent prediction of explosion phenomena therefore requires spatially resolved modeling that accounts for both energy and molecular transport processes.

ARTICLE HISTORY
Received 17 June 2026
Revised 21 August 2026
Accepted 12 September 2026

KEYWORDS
Explosion limit; hydrogen-oxygen; ignition process; transport processes; surface reaction

CONTACT Chunkan Yu chunkan.yu@kit.edu Institute of Technical Thermodynamics, Karlsruhe Institute of Technology, Engelbert-Arnold-Straße 4, Karlsruhe D-76131, Germany

Introduction

Explosion limits of hydrogen mixtures and spatially resolved modeling

With the global push toward carbon neutrality, hydrogen is considered as a promising potential component of the future energy system for achieving zero-carbon emissions. However, hydrogen is also a highly flammable and diffusible gas, presenting notable safety challenges during its storage, transport, and utilization (Wen et al. 2025). Among these, the explosion behavior of hydrogen has attracted significant attention, as it shows potential hazards that must be carefully managed. Therefore, a comprehensive understanding and accurate modeling of hydrogen's explosion characteristics, especially its explosion limits under varying conditions, is essential for the safe and large-scale deployment of hydrogen energy technologies. In predicting explosion limits, several parameters such as temperature and system pressure have been identified as key factors influencing the explosion limits of hydrogen-oxygen-nitrogen mixtures (Heiple and Lewis 1941; von Elbe and Lewis 1942; Maas and Warnatz 1988; Lee and Hochgreb 1998). These factors can significantly alter the boundaries of explosion limits and affect the quantitative assessment of explosion risks. Accurately identifying and modeling the influence of these variables is therefore critical not only for understanding the fundamental explosion mechanisms of hydrogen but also for improving predictive accuracy and informing engineering safety strategies.

Since the discovery of the three explosion limits in hydrogen–oxygen mixtures in the 1930s and 1940s, numerous efforts have been made to quantitatively explain this complex phenomenon (Heiple and Lewis 1941; von Elbe and Lewis 1942). However, many of these attempts required significant simplifications in order to make the problem solvable. Such simplifications include the reduction of reaction mechanisms, the application of quasi-steady-state assumptions, or the restriction of the analysis to zero-dimensional systems. For example, the quasi-steady-state assumption was applied for intermediate species such as HO_2, H, and H_2O_2 in (von Elbe and Lewis 1942). Moreover, by recognizing the significant differences in chemical reaction rates under varying pressures and temperatures, the three explosion limits were analyzed separately. While such approaches provided valuable insights into the fundamental behavior of hydrogen combustion, they also introduced limitations that affect the accuracy and generalizability of the resulting predictions.

Importantly, the role of transport processes in hydrogen-oxygen explosion limits has long been recognized. Early studies already considered the influence of H-atom diffusion on the first explosion limit (Kassel and Storch 1935), while subsequent theoretical and numerical investigations examined the effects of molecular transport on different explosion regimes. In particular, the influence of H2O2 diffusion under conditions associated with the third explosion limit has also been investigated (Sánchez et al. 2014). Furthermore, Maas and Warnatz (1988) applied the one-dimensional mathematical model including the molecular and energy transports to find out the explosion limit.

Homogeneous modeling approaches

Nevertheless, many recent numerical investigations of explosion limits have returned to homogeneous reactor formulations (Wang and Law 2013; Liang and Law 2018; Wang et al. 2024; Li et al. 2025). While such models provide an efficient framework for kinetic analysis, spatial gradients in temperature and species concentrations, and hence the associated

energy and molecular transport processes, are not explicitly resolved. For the homogeneous modeling approaches, these simulations rely heavily on the following assumptions (Wang and Law 2013; Liang and Law 2018; Wang et al. 2024; Li et al. 2025):

- the diffusion of radicals toward the reactor wall is much faster than their absorption by the wall, and
- the concentrations of radicals at the wall are the same as those in the gas phase

Furthermore, the destruction of radicals at the wall surface is calculated using sticking coefficients, the surface area-to-volume ratio, and the temperature-dependent average velocity of the thermal motion of the radicals (Wang and Law 2013). In this way, the entire process is typically formulated as a system of ordinary differential equations (ODEs). However, such models often lack a clear sudden sharp increase in thermo-kinetic states which can indicate the occurrence of an explosion. As a result, the definition of explosion in these works tends to be rather intuitive or empirical. For example, an explosion may be defined as a temperature increase of 50 K within 10 seconds (Liu et al. 2018; Wang et al. 2024), or as the consumption of 50% of the initial hydrogen within 0.1 seconds (Li et al. 2025). Consequently, the predicted explosion limits may depend on the selected criterion, and suitable empirical thresholds can yield good agreement with experimental explosion measurement. A direct comparison between such predictions and the present spatially resolved results would therefore not provide a clear assessment on the role of transport. In the present model, by contrast, explosion is identified from the sharp thermo-kinetic transition emerging naturally from the calculated temporal and spatial evolution, without introducing such an empirical threshold. More importantly, the absence of spatial gradients in temperature and species concentrations in homogeneous systems prevents these models from capturing key physical processes. For example, hydrogen diffusion plays a critical role in determining the first explosion limit, while heat losses to the wall surface are essential for accurate prediction of the third explosion limit, both of which cannot be adequately resolved in homogeneous frameworks.

Scope and purpose of the present work

Although most recent studies employ homogeneous reactor models, it is worth noting that a spatially resolved description of hydrogen explosion limits was already introduced in the 80s (Maas and Warnatz 1988, 1989). By solving time-dependent one-dimensional partial differential equations, the model incorporated detailed chemical kinetics, multicomponent molecular transport, and realistic surface reactions, thereby avoiding many of the simplifying assumptions commonly adopted in both earlier and more recent studies. The resulting simulations successfully reproduced the experimentally observed explosion limits and showed that the onset of explosion can be identified naturally by a sharp thermo-kinetic transition.

The present work does not aim to reproduce these established results, nor to claim the individual transport effects considered here as previously unknown. Instead, building upon the spatially resolved framework of Maas and Warnatz (1988, 1989), the objective is to systematically clarify the physical importance of energy and molecular transport and the

associated spatial inhomogeneities. In particular, the following key scientific questions are addressed:

- how do wall heat losses quantitatively influence the different explosion limits, in particular the thermally controlled third limit;
- to what extent do molecular transport processes, including thermal diffusion and differential diffusion of radicals, affect both ignition and post-ignition dynamics; and
- how do spatial inhomogeneities in temperature and species concentrations modify the transition between non-explosive and explosive regimes.
- do homogeneous models represent an accurate description?

To answer these questions, a one-dimensional spatially resolved model is used to systematically investigate energy and mass transport effects in stoichiometric hydrogen–oxygen mixtures. By solving the one-dimensional governing equations, we investigate how species diffusion and wall heat conduction affect the transition between non-explosive and explosive regimes. In particular, we have incorporated a simplified wall heat transfer model to account for heat loss at the vessel boundary, which allows the model to capture the influence of wall conduction on the explosion process, especially for the third explosion limit. Furthermore, the effects of thermal diffusion (Soret effect) and differential diffusion of radicals are analyzed, providing a comprehensive assessment of how inhomogeneities in temperature and species concentrations impact the occurrence of explosion regimes.

Mathematical modeling

Brief outline of the governing equations

Following (Maas and Warnatz 1988), the governing equations are transformed from Eulerian to Lagrangian coordinates using $\psi(r,t) = \int_0^r r^2\rho(r,t)\mathrm{d}r$, where r denotes the radial coordinate, t the time, and ρ the mixture density. The use of the Lagrangian coordinate ψ eliminates the convection terms from the governing equations, while the continuity equation is automatically fulfilled. Under the additional assumption of spatially uniform pressure, the resulting system consists of the transport equations for the species mass fractions $w_i = w_i(t,\psi)$ Eq.(3), the temperature $T = T(t,\psi)$ Eq.(4), the metric transformation equation Eq.(1), and the ideal-gas law Eq.(5):

$$\frac{\partial r}{\partial \psi} - \frac{1}{\rho r^2} = 0 \tag{1}$$

$$\frac{\partial p}{\partial \psi} = 0 \tag{2}$$

$$\frac{\partial w_i}{\partial t} + \frac{\partial}{\partial \psi}\left(r^2 j_i\right) - \frac{\dot{\omega}_i M_i}{\rho} = 0 \tag{3}$$

$$\frac{\partial T}{\partial t}-\frac{1}{\rho c_p}\frac{\partial p}{\partial t}-\frac{1}{c_p}\frac{\partial}{\partial \psi}\left(\rho r^4\lambda\frac{\partial T}{\partial \psi}\right)+\frac{r^2}{c_p}\sum_{i=1}^{n_s}j_i c_{pi}\frac{\partial T}{\partial \psi}+\frac{1}{\rho c_p}\sum_{i=1}^{n_s}\dot{\omega}_i h_i M_i=0 \tag{4}$$

$$p-\frac{\rho RT}{\bar{M}}=0 \tag{5}$$

In these equations, c_p = isobaric specific heat capacity of the mixture, λ = heat conductivity of the mixture, n_s = number of species, M_i = molar mass of species i, h_i = specific enthalpy of species i, $\dot{\omega}_i$ = molar formation rate of species i, c_{pi} = isobaric heat capacity of species i. j_i represents the total diffusion mass flux including the differential diffusion part j_i^d and thermal diffusion part (Soret effect) j_i^T:

$$j_i=j_i^d+j_i^T=-\rho D_i^D\frac{w_i}{x_i}\frac{\partial x_i}{\partial r}-\frac{D_i^T}{T}\frac{\partial T}{\partial r}=-\rho r^2\left(\rho D_i^D\frac{w_i}{x_i}\frac{\partial x_i}{\partial \psi}-\frac{D_i^T}{T}\frac{\partial T}{\partial \psi}\right) \tag{6}$$

in which D_i^D and D_i^T are the molecular diffusion coefficients and thermal diffusion coefficient (Hirschfelder et al. 1964; Maas and Warnatz 1988). Further details of the coordinate transformation and the derivation of the governing equations are given in (Maas and Warnatz 1988).

It can be clearly seen that the governing equations explicitly account for both energy and species mass transport through the heat-conduction and species-diffusion terms. Consequently, spatial gradients in temperature and species concentrations are directly resolved, allowing the model to capture the resulting inhomogeneities within the reactive mixture. This is particularly important for explosion-limit calculations, since phenomena such as wall heat loss, radical diffusion and flame propagation are inherently governed by spatial transport processes. Owing to the spherical symmetry of the reactor, these effects can be represented within a one-dimensional framework while retaining the essential physical mechanisms. The present formulation therefore provides a physically consistent description of transport-controlled explosion phenomena without introducing the additional complexity of multi-dimensional simulations.

Computational domain and boundary conditions

Initial condition

For the initial condition, the fields of reactant concentrations and temperatures are homogeneously distributed, indicating an initially uniform reacting system:

$$T(\psi,t=0)=T_0,\quad w_i(\psi,t=0)=w_{i,0}. \tag{7}$$

Inner boundary

Because the solution is restricted to the radial coordinate from the center to the wall, the center of the reactor ($r=0$, or $\psi=0$ in Lagrangian coordinate) becomes the origin of the computational domain (as shown in Figure 1), where radial symmetry conditions are applied:

$$r(\psi=0,t)=0,\left.\frac{\partial T}{\partial r}\right|_{r=0,t}=\left.\frac{\partial w_i}{\partial r}\right|_{r=0,t}=0, \tag{8}$$

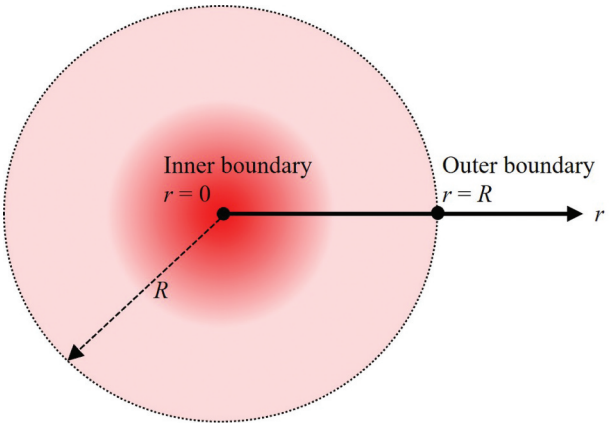

Figure 1. Physical structure for the calculation area.

or expressed in Lagrangian coordinate as:

$$\left.\frac{\partial T}{\partial \psi}\right|_{\psi=0,t} = \left.\frac{\partial w_i}{\partial \psi}\right|_{\psi=0,t} = 0. \tag{9}$$

Note that here both the temperature gradient and the concentration gradient are zero, which means that the diffusion mass flux of species i is also zero $j_i = 0$ according to.

Outer boundary

The outer boundary is located at the vessel surface, corresponding to $r = R$ (or $\psi = \psi^s$ in Lagrangian coordinate), in which R is the radius of the cylindrical vessel (c.f. Figure 1).

For the boundary condition of the species, both the total diffusive mass flux () and the surface flux due to surface reactions ($\dot{\omega}_i^s$) must be taken into account. Consequently, the total mass flux of species i vanishes at the surface, which is formulated as:

$$j_i(\psi^s, t) + M_i\dot{\omega}_i^s = 0, \tag{10}$$

The consideration of heat conduction through the vessel wall provides the boundary condition for the energy equation. That is, at the wall surface, the heat flux on the gas side $j_q^{\text{Gas}}(\psi^s, t)$ must be equal to the heat flux conducted through the vessel wall j_q^{Wall}:

$$j_q^{\text{Gas}}(\psi^s, t) = j_q^{\text{Wall}}. \tag{11}$$

The heat flux on the gas side $j_q^{\text{Gas}}(\psi^s, t)$ consists of two contributions: one term is the conductive heat flux according to the Fourier's law, and the other term is the diffusion-related contribution, which accounts for the enthalpy transport caused by the diffusion of species with different specific enthalpies. Thus, it can be written as:

$$j_q^{\text{Gas}}(\psi^s, t) = -\lambda\frac{\partial T}{\partial r}\Big|_{\psi^s,t} + \sum_{i=1}^{n_s} h_i j_i(\psi^s, t) \; = -\lambda\rho r^2\frac{\partial T}{\partial r}\Big|_{\psi^s,t} + \sum_{i=1}^{n_s} h_i j_i(\psi^s, t) \tag{12}$$

The heat flux conducted through the vessel wall, j_q^{Wall}, can be approximated by introducing the concept of thermal insulance R_T in unit $\text{m}^2 \cdot K/\text{W}$ or, equivalently, thermal transmittance $U = 1/R_T$:

$$j_q^{\text{Wall}} = \frac{T(\psi^s, t) - T_0}{R_T} = U(T(\psi^s, t) - T_0). \tag{13}$$

Here, we consider the colder temperature as T_0, the initial temperature, which is a reasonable setup since in experiments (von Elbe and Lewis 1942) both the reactor and the gas mixture are uniformly heated to this given temperature before observing whether an explosion occurs or not by varying pressures.

Chemical mechanism

In the present work, the chemical mechanism is adopted from (Maas and Warnatz 1988), which has showed high accuracy in predicting all explosion limits when compared to experimental measurements. This chemical mechanism consists of 8 reactive species and 19 reversible elementary reactions. Reactive species involve H_2, O_2, H, O, OH, H_2O_2, HO_2 and H_2O. The corresponding Arrhenius parameters can be found in (Maas and Warnatz 1988).

Reactions at the wall surface

As reported in various publications (Clark et al. 1970; Maas and Warnatz 1988; Wang and Law 2013), surface reactions at the vessel wall may play an important role in the auto-ignition process within a closed vessel at relative low pressures. These surface reactions involve recombination of atoms or destruction of reactive molecules at the surface (e.g. $H \xrightarrow{\text{wall}} 0.5\,H_2$), serving as chain termination steps. In the present work, a simple surface reaction model (neglecting species accumulation at the wall surface) described in (Maas and Warnatz 1988) is used, which can be symbolic expressed as:

$$a_{lk}\text{A}_l \longrightarrow \tilde{a}_{1k}\text{A}_1 + \tilde{a}_{2k}\text{A}_2 + \cdots \tilde{a}_{n_s k}\text{A}_{n_s}, \tag{14}$$

in which a_{ik} is the stoichiometric coefficient of species i in reaction k from the reactant side (without $\tilde{\cdot}$) and from the product side (with $\tilde{\cdot}$). For such surface reaction, the mass rate of formation of species i per surface unit due to the surface reaction can be determined as

$$\dot{\omega}_i^s = \sum_{k=1}^{n_s} \gamma_k Z_l M_i \{\tilde{a}_{ik} - \delta_{li} a_{lk}\}, \tag{15}$$

where γ_k is the surface destruction efficiency for surface reaction k. Z_l is the surface collision number of species l, which can be calculated as (Bird et al. 2002):

$$Z_l = \frac{1}{4}\sqrt{\frac{8RT}{\pi M_l}} c_l, \tag{16}$$

with R the universal gas constant, and c_l the volumetric mole concentration of species l. A more detailed modeling for surface reaction including the determination of mass rate of

formation of species i per surface unit due to the surface reaction can be found in (Maas and Warnatz 1988).

The surface reactions used in this work involve five highly reactive species found in hydrogen combustion chemistry, namely H, O, OH, HO2, and H2O2 radicals, and are consistent with those in (Maas and Warnatz 1988):

$$(\mathrm{S1})\mathrm{HO_2} \xrightarrow{\text{wall}} 0.5\mathrm{H_2O} + 0.75\mathrm{O_2}$$

$$(\mathrm{S2})\mathrm{O} \xrightarrow{\text{wall}} 0.5\mathrm{O_2}$$

$$(\mathrm{S3})\mathrm{H} \xrightarrow{\text{wall}} 0.5\mathrm{H_2}$$

$$(\mathrm{S4})\mathrm{OH} \xrightarrow{\text{wall}} 0.5\mathrm{H_2O} + 0.25\mathrm{O_2}$$

$$(\mathrm{S5})\mathrm{H_2O_2} \xrightarrow{\text{wall}} \mathrm{H_2O} + 0.5\mathrm{O_2}$$

These surface reactions act primarily as chain-termination pathways by removing reactive radicals from the gas phase. Therefore, surface reactions can influence the competition between radical production and termination, particularly under low-pressure conditions near the first explosion limit (see discussion later). Additionally, it is important to emphasize that the choice of the stable species into which these radicals are converted at the surface is not critical. What matters is the inclusion of surface reactions which destroy radicals. In other words, numerical experiments show that reactions such as $\mathrm{HO2} \xrightarrow{\text{wall}} 0.5\mathrm{H2O} + 0.75\mathrm{O2}$ and $\mathrm{HO2} \xrightarrow{\text{wall}} 0.5\mathrm{H2} + \mathrm{O2}$ yield equivalent results in terms of explosion behavior.

Numerical setup

All numerical conditions in the present study are chosen consistently with those used in (Maas and Warnatz 1988), namely a stoichiometric hydrogen–oxygen mixture inside a spherical reactor with a radius of 3.7 cm. For the surface reactions, a surface destruction efficiency of $\gamma_i = 1 \times 10^{-3}$ is used, which has been experimentally validated in (Maas and Warnatz 1988). This setup ensures that the present simulations are based on a physically verified reference case, allowing us to focus on analyzing and isolating the influence of transport phenomena on the underlying explosion behavior.

Definition of explosion limits

Before further discussing how different parameters or model assumption affect the calculated explosion limits, it is essential to first provide a clear definition of an explosion. In other words, we must distinguish between conditions under which no explosion occurs and those that result in an explosion. As previously mentioned, in several recent publications involving calculating explosion limits using a homogeneous reactor model, an explosion is often defined as a temperature increase of 50 K within 10 seconds (Liu et al. 2018; Wang et al. 2024) or the consumption of 50% hydrogen within 0.1 seconds (Li et al. 2025).

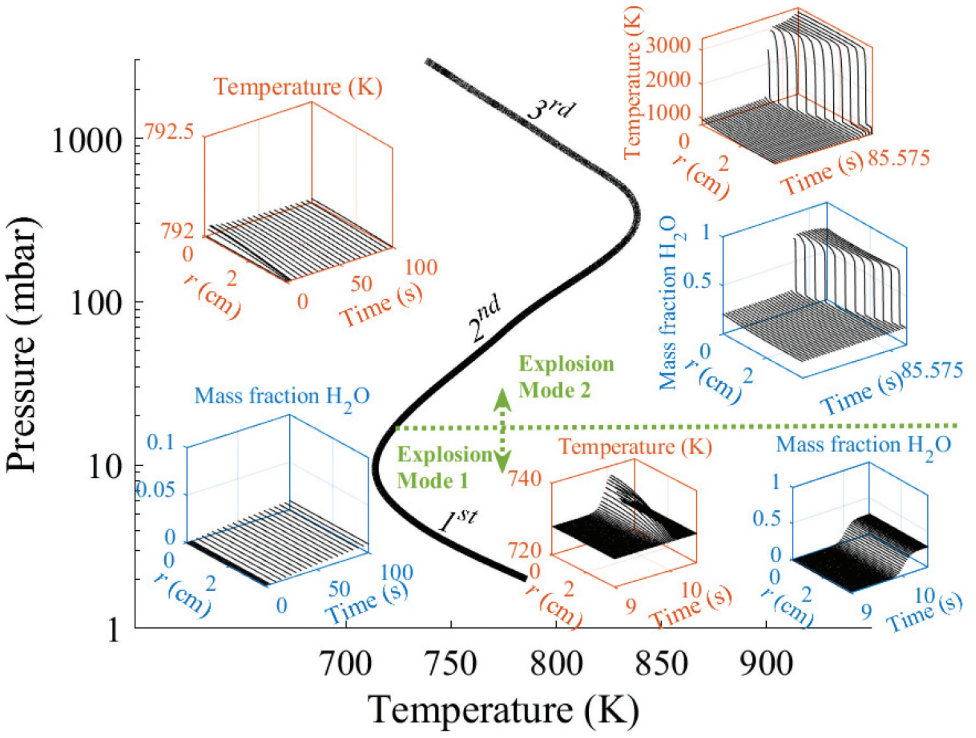

Figure 2. Calculated explosion limits for stoichiometric hydrogen-oxygen mixtures. Red frames: temperature development; blue frames: mass fraction of H_2O development. Left of the curve: non-explosion regime; right of the curve: explosion regime.

However, as we will show below, defining explosion solely based on a specific temperature increase or fuel conversion is inherently arbitrary and becomes particularly problematic at very low pressures, where the temperature change is often minimal.

Figure 2 presents the calculated explosion limits for stoichiometric hydrogen–oxygen mixtures (The quantitative definition of ignition used in this work is provided in the subsequent subsections.). To clearly illustrate the occurrence of explosion, representative temporal evolutions of temperature (red frames) and the mass fraction of H2O (blue frames) under different conditions are also included in this figure.

For the non-explosive regime (i.e., to the left of the explosion limit curve), both temperature and H2O mass fraction remain nearly constant over the entire 100 ms observation period. Within the explosive regime (to the right of the curve), two different explosion modes can be identified: i) Explosion mode 1 corresponds to very low-pressure conditions (the first explosion limit), and ii) Explosion mode 2 occurs at moderate to high pressures (the second and third explosion limits). Both will be discussed in details in the following two sub-sections.

Explosion behavior at the first explosion limit (very low pressure)

Under very low-pressure conditions, relying solely on the temperature development to determine whether an explosion has occurred is not an appropriate criterion. Figure 3 (left

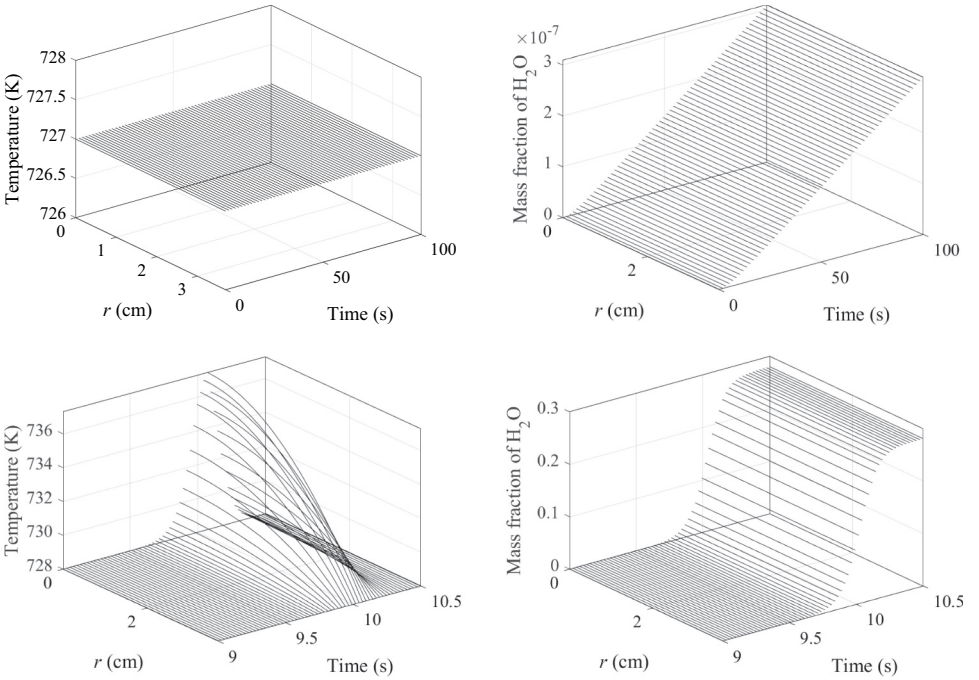

Figure 3. Calculated transient profiles for temperature and mass fraction of H_2O for the stoichiometric hydrogen-oxygen mixture at initial pressure $p = 5$ mbar (at the first explosion limit). Upper for a failed explosion with $T_0 = 727$ K; below for a successful explosion with $T_0 = 728$ K. Note difference in z-axis scale. For reasons of visual clarity, not all time steps are displayed.

two sub-figures) shows the temporal evolution of temperature during the ignition of a stoichiometric H2-O2 mixture at a pressure of 5 mbar, corresponding to the first explosion limit. It is clearly observed that for an initial temperature of 727 K (upper left subfigure), the system temperature remains almost unchanged over the entire 100 second period. However, when the initial temperature is increased by just 1 K to 728 K (lower left subfigure), the maximum temperature in the system rises by approximately 9 K, which is still a minor increase. Subsequently, due to heat loss induced by the temperature gradient at the wall surface, the system temperature returns to its initial value. Therefore, if one follows the criterion commonly proposed in the literature such as in Liu et al. (2018); Liang and Law (2018); Wang et al. (2024),namely identifying an explosion based on a certain temperature rise within the system (e.g. 50 K), then neither of the two initial conditions would be classified as having led to an explosion. However, upon further observation of the mass fraction of H2O as the major reaction product, it becomes evident that its formation differs significantly between these two initial temperature conditions. At an initial temperature of 727 K (upper right subfigure), the H2O mass fraction remains at a very low level even after 100 seconds. In contrast, when the initial temperature is increased to 728 K (lower right subfigure), a sudden rise in the H2O mass fraction is observed within a short time range. This indicates that, although the corresponding temperature increase in the system is only slight (i.e. approximately 9 K increase), a large amount of H2O is rapidly generated through chemical reactions. From this example, it becomes clear that under very low pressure

conditions (namely first explosion limit), temperature is not a reliable indicator for identifying an explosion. Even a minor temperature change may be accompanied by a significant production of the major product, H2O, indicating that chemical activity has occurred despite the limited thermal response inside the system.

Explosion behavior at the second and third explosion limit (moderate and high pressure)

In this regime, the onset of explosion is clearly characterized by a sharp rise in system temperature, accompanied by a rapid and substantial production of H2O. The mixture self-ignites at the center of the vessel. Subsequently, a well-defined flame front develops and propagates outward through the reactor. Importantly, in the present spatially resolved framework, the occurrence of explosion can be identified directly from this sharp thermo-kinetic transition, without the need for an artificial or empirical criterion (such as prescribing a specific temperature rise within a given time interval in (Liu et al. 2018; Wang et al. 2024)). The explosion is therefore determined based on the intrinsic physical behavior of the system, rather than on a pre-defined threshold definition as commonly adopted in homogeneous models.

By accounting for spatial inhomogeneities in temperature and species concentrations, the flame propagation can also be determined in a physically consistent manner additionally. For an outwardly propagating spherically symmetric flame, the stretched flame speed is defined as $S_{\mathrm{L,b}} = \mathrm{d}R_f/\mathrm{d}t$, where R_f denotes the flame front position, identified here by the location of the peak heat release rate. Plotting $S_{\mathrm{L,b}}$ against the stretch rate $K = (2/R_f) \cdot \mathrm{d}R_f/\mathrm{d}t$ allows the un-stretched flame speed ($K = 0$) to be estimated via linear regression (Giannakopoulos et al. 2015; Beeckmann et al. 2017). As shown later, although molecular transport has only a minor influence on the explosion limits at moderate and high pressures, it significantly affects the post-ignition flame propagation process. Therefore, using the knowledge of (un)stretched flame speed is essential to discuss flame propagation after explosion.

As the flame approaches the reactor wall, the large temperature gradient induces additional heat loss. This further highlights the importance of temperature inhomogeneity: a homogeneous model cannot capture wall heat loss or the competition between heat release and heat dissipation. This aspect is examined in more detail in the following sections.

General definition for an explosion

Based on the above examples, in the cases of the second and third explosion limits, the occurrence of an explosion can be simply identified by a sharp increase in the system temperature. However, for the first explosion limit, the temperature increase is often relatively small (e.g., around 10 K). Therefore, using the temperature change alone to define whether an explosion has occurred is not sufficient to cover all explosion limits comprehensively. Nevertheless, for all three explosion limits, the occurrence of an explosion is typically accompanied by a significant production of the major product, which in the present work is H2O. Therefore, considering the generation of the major product provides

a more robust indicator for determining whether an explosion has occurred in the system. It should be noted that in the work by Li et al. Li et al. (2025), the explosion limit is also determined based on species rather than temperature. However, their ignition criterion (defined as the state at which 50% of hydrogen is consumed) is rather arbitrary. In our case, if a sudden increase of H_2O production is observed if initial temperature is increased by 1 K at a certain initial pressure, then an explosion limit is obtained for this initial pressure.

Results and discussion

In this section, the influence of energy and molecular transport processes on the explosion limits is systematically analyzed. Particular emphasis is placed on identifying how wall heat loss and species diffusion modify the transition between non-explosive and explosive regimes. First, the role of heat transfer at the reactor wall is examined to clarify the thermal nature of the third explosion limit. Subsequently, the effects of molecular transport are investigated in detail, including thermal diffusion as well as the differential diffusion of key radicals (H and H2O2). Through this analysis, the relative importance of transport phenomena in determining explosion behavior is investigated.

Influence of heat loss at wall surface

Under high-pressure conditions (such as those corresponding to the third explosion limit), the classical theory attributes the transition from non-explosive to explosive behavior to the competition between heat release and heat loss at the wall (Zeldovich et al. 1985; Warnatz et al. 2006; Williams 2018). Therefore, under such conditions, accounting for heat loss at the wall is important for achieving accurate modeling results. However, in many recent publications such as (Liu et al. 2018; Wang et al. 2024; Li et al. 2025), the interpretation of the third explosion limit has primarily focused on chemical effects, as these studies used homogeneous models. In such models, there is no temperature gradient at the wall, and the entire system is approximated as adiabatic. This contradicts the classical understanding, in which thermal losses are considered essential for explaining the behavior near the third explosion limit.

Stoichiometric mixture condition

Figure 4 presents the classical $p - T$ explosion diagram, where four curves correspond to simulations using four different thermal transmittance values (or, equivalently, thermal insulances). The black solid line represents the case with a fixed temperature at the wall surface, corresponding to a Dirichlet boundary condition and a thermal insulance of $R_T = 0$. The blue solid line corresponds to $R_T = \infty$, meaning zero heat flux at the boundary ($j_q = 0$), which represents an adiabatic boundary condition. The two other colored dashed lines represent cases with two intermediate values of thermal insulance. It is clearly observed that the first and second explosion limits remain unaffected by changes in thermal insulance. However, the third explosion limit shows a strong sensitivity to thermal insulance.

To better illustrate how the temperature required for explosion T_{Ex} (i.e., the minimum temperature at a given pressure that leads to explosion) varies with thermal transmittance U

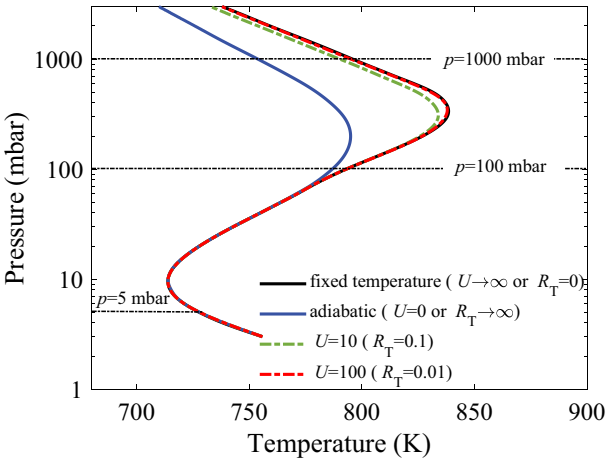

Figure 4. Influence of different values of thermal insulance R_T for temperature boundary conditions on the $p - T$ explosion diagram. Stoichiometric hydrogen-oxygen mixture is considered.

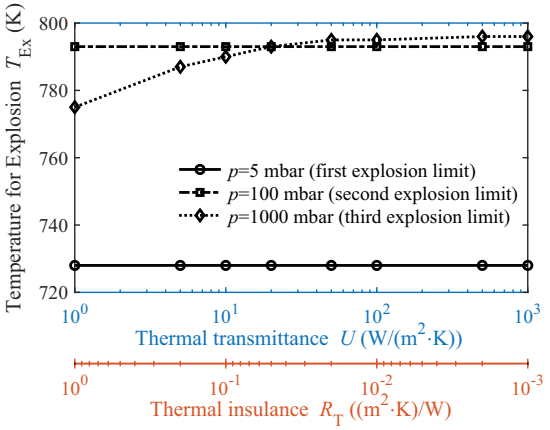

Figure 5. Influence of different values of thermal insulance R_T for temperature boundary conditions on explosion temperature at three different pressures. Three conditions are selected as representative conditions for three different explosion limits and shown in the same figure due to space limit.

or thermal insulance R_T, Fig. 5 considers three different pressures, each representative of one of the explosion limits. It can be seen that first and second explosion limits remain invariant with respect to changes in thermal transmittance. As discussed in many other studies (Maas and Warnatz 1988; Lewis and Von Elbe 2012; Wang and Law 2013), the key factors determining whether an explosion occurs at first and second explosion limits are chemically controlled, and there exists a competition between chain-branching and chain-termination reaction steps, and the thermal losses at the wall surface have no significant effect on both explosion limits.

However, as the pressure increases and reaches the third explosion limit, a strong influence of the thermal transmittance U (or the thermal insulance R_T) on the explosion behavior is observed. As shown in Figure 5, the temperature required

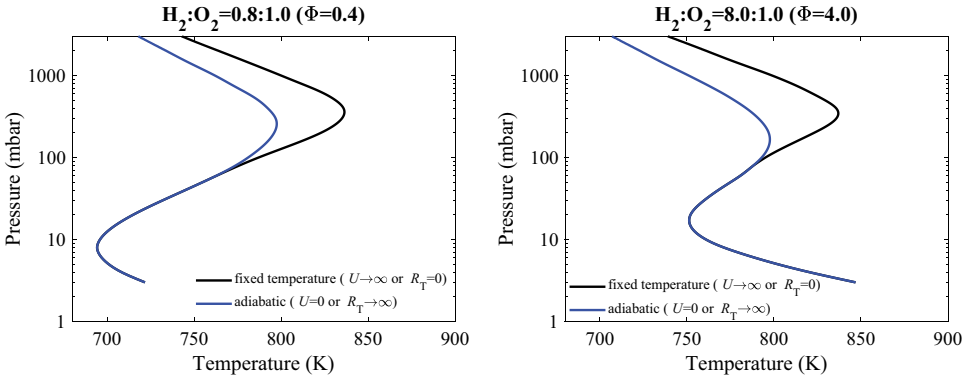

Figure 6. Calculated explosion limits for hydrogen-oxygen mixtures under lean condition ($\Phi = 0.4$, left sub-figure) and under rich condition ($\Phi = 4.0$, right sub-figure) for fixed temperature (black lines) and adiabatic boundary conditions (blue lines). Color lines are consistent as the lines in Figure 4.

for explosion T_{Ex} increases monotonically with thermal transmittance U. This agrees with the classical interpretation (Warnatz et al. 2006; Lewis and Von Elbe 2012; Williams 2018) that the third explosion limit is a thermal explosion governed by the competition between heat release and wall heat loss. A smaller U (or a larger R_T) implies better insulation, resulting in a smaller temperature gradient at the wall and reduced heat loss ($-\lambda dT/dr$). In the limit $U \to 0$ (or $R_T \to \infty$), the system becomes nearly adiabatic, retaining all released heat within the mixture, which causes a rapid temperature rise and explosion. The noticeable influence of heat loss at the wall in the third explosion limit directly indicates the importance of the temperature-field inhomogeneity. The temperature gradient near the wall plays a decisive role in accurately capturing the thermal losses from the gas phase, whereas simplified homogeneous approaches fail to account for such important thermal effects that govern the occurrence of explosion under high-pressure conditions (third explosion limit).

Lean and rich mixture conditions

To study whether the influence of wall heat loss discussed above is limited to the stoichiometric mixture, additional calculations are performed for lean ($\Phi = 0.4$) and rich ($\Phi = 4.0$) conditions. Figure 6 compares the calculated explosion limits using fixed-temperature (black solid lines) and adiabatic boundary conditions (blue solid lines). For both lean and rich mixtures, the same general behavior as that observed for the stoichiometric mixture is obtained. Especially, a pronounced difference is observed near the third explosion limit if different thermal boundary conditions are used. In particular, the adiabatic boundary condition significantly shifts the third explosion limit to the lower temperature regime compared with the fixed-temperature condition. These results suggest that the strong sensitivity of the third explosion limit to wall heat loss is not restricted to the stoichiometric mixture, but persists over a wider range of mixture compositions. This further supports the importance of explicitly resolving wall heat transfer and the associated temperature inhomogeneity when modeling the third explosion limit.

Influence of molecular transport

Molecular transport strongly influences the spatial distribution of radicals within the reactive mixture. To assess its role, this section studies the effects of thermal diffusion and the diffusion of key radicals (especially H and H2O2) on the explosion behavior.

Before examining the thermal diffusion and the diffusion of individual species in detail, it is useful to first compare the detailed transport model with two commonly used simplified transport formulations:

- *Unity Le model*

$$d = \frac{\lambda}{\rho c_p}, \tag{17}$$

in which the gas mixture has the heat conductivity λ, density ρ and isobaric heat capacity c_p.

- *Differential diffusion model without thermal diffusion:*

$$j_i = j_i^d. \tag{18}$$

Note that for both models, the heat conductivity of gas mixtures is calculated in an exact way which is temperature dependent.

Figure 7 shows the computed explosion limits for stoichiometric hydrogen-oxygen mixtures using different molecular transport models. The black solid line represents results obtained with a detailed transport model that includes thermal diffusion. The green dashed line corresponds to the model that accounts for differential diffusion but neglects thermal diffusion. The red dashed line represents the results using a transport model with a unity Lewis number. This comparison provides an overall assessment of the importance of molecular transport modeling for the prediction of explosion limits. However, it does not

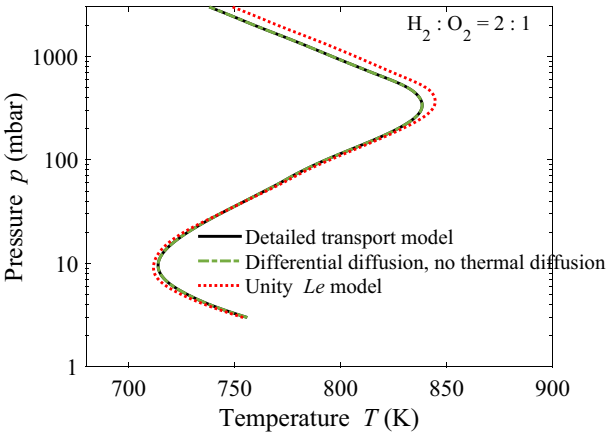

Figure 7. Calculated explosion limits for hydrogen-oxygen mixtures with H_2:O_2 = 2:1 with different molecular diffusion transport models.

identify which individual transport processes or species are responsible for the observed differences. Therefore, the following subsections separately discuss the role of thermal diffusion and the differential diffusion of key reactive species, particularly H and H_2O_2.

Influence of thermal diffusion

Numerical simulations show that thermal diffusion has no effect on the p–T explosion diagram for the conditions considered here.

This is primarily because the initiation of ignition, which determines whether an explosion occurs, is governed mostly by the accumulation of highly reactive radicals (cf. Figure 2). In the early stage, the system undergoes a radical buildup process similar to classical autoignition: chain-branching reactions slowly increase the radical pool while the overall temperature rises only slightly. During this induction period, the temperature change is very small and, consequently, temperature gradients within the system remain weak, leading to negligible thermal diffusion effects. Since thermal diffusion is driven by temperature gradients, its contribution during this radical-accumulation phase is insignificant for determining the onset of explosion.

Influence of diffusion flux of H radical

Figure 8 shows the effect of varying the diffusion flux of H radicals (j_H) on the p–T explosion diagram. Consistent with previous study (Maas and Warnatz 1988), j_H influences only the first explosion limit, while the second and third remain unaffected. At the first limit, increasing j_H has little impact on the explosion temperature, whereas reducing it markedly extends the explosion region. The reason is straightforward: a smaller j_H slows the transport of H radicals to the wall, allowing more radicals to remain in the gas phase and promote chain-branching reactions (especially H+O2 → OH+O), thus favoring explosion. In contrast, when j_H is increased, surface reaction becomes rate limiting, so the overall explosion behavior remains nearly unchanged.

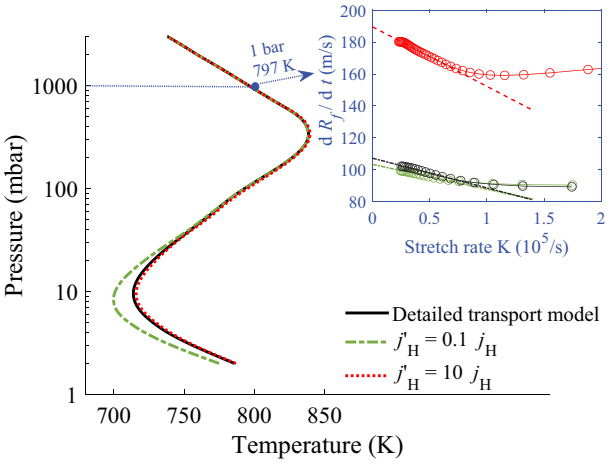

Figure 8. Influence of different diffusion flux of H radical j_H on the $p-T$ explosion diagram of stoichiometric hydrogen-oxygen mixture. Both figures share the same legend.

Although variations in the diffusion flux of H radicals have no influence on the second and third explosion limits, they do affect the subsequent flame propagation toward the wall once ignition has occurred. Therefore, the upper-right panel of Fig. 8 presents the stretched flame propagation speed $S_{L,b}$ plotted against the stretch rate K for an outwardly propagating spherically symmetric flame at $p = 1$ bar and $T_0 = 797$ K (corresponding to the condition slightly above the third explosion limit). The dashed line represents a linear regression used to estimate the unstretched flame speed ($K = 0$) (Giannakopoulos et al. 2015; Beeckmann et al. 2017). It should be noted that the objective here is not to determine an exact laminar flame speed, but to discuss the relative sensitivity of flame propagation to molecular transport parameters. However, this procedure is analogous to the methodology commonly used in constant-volume combustion-bomb experiments, where the propagation speed of an outwardly propagating spherical flame is determined from the temporal evolution of the flame radius. Therefore, the present spatially resolved simulations allow to be directly related to experimentally determined spherical flame propagation characteristics.

The results clearly show that, although modifying j_H does not shift the explosion limit itself, it significantly alters the flame propagation speed after successful ignition. Increasing the diffusion flux by one order of magnitude leads to an overestimation of the propagation velocity by approximately a factor of two. This observation highlights an important point: incorporating a physically consistent molecular transport model not only enables accurate prediction of explosion limits, but also allows a realistic description of the post-ignition flame dynamics. Such consistency is essential from a physical standpoint, since explosion onset and subsequent flame propagation are governed by the same coupled processes of chemistry and transport. A model that neglects or oversimplifies molecular diffusion may still reproduce certain explosion limits, but it cannot reliably capture the full physical evolution of the system once ignition occurs.

Influence of diffusion coefficient of H_2O_2 radical

Figure 9 illustrates the influence of varying the mass diffusion flux of H2O2 on the p–T explosion diagram. It can be clearly seen that the diffusion flux of H2O2 affects only the third explosion limit, while the first and second explosion limits remain essentially unchanged. Specifically, for the same pressure corresponding to the third explosion limit, a larger diffusion flux (i.e., faster diffusion of H2O2) requires a higher temperature to initiate explosion.

This behavior can be explained by the fact that, under high-pressure conditions, the reaction sequences via $H+O_2+M \rightarrow HO_2+M$, $HO_2+H_2 \rightarrow H_2O_2+H$ and $H_2O_2+M \rightarrow OH+OH+M$ plays a significant chain-branching role in initiating the explosion. Consequently, the local concentration of H2O2 in the reactive region strongly influences the onset of ignition. When the diffusion of H2O2 is enhanced, more H2O2 diffuses away from the central region, effectively lowering its concentration where this branching step occurs. This weakens the formation and accumulation of OH radicals, thereby suppressing chain-branching activity and delaying the onset of explosion. Since H2O2-related reactions are particularly important near the third explosion limit, this effect manifests only in this regime, while the lower- and moderate-pressure limits remain unaffected.

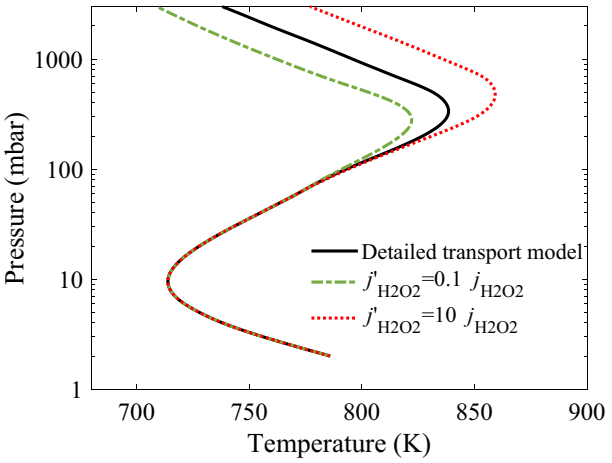

Figure 9. Influence of different diffusion coefficient of H_2O_2 radical D_{H2O2} on the $p-T$ explosion diagram of stoichiometric hydrogen-oxygen mixture.

Sensitivity of elementary reactions to modified diffusion fluxes

To further study the coupling between molecular transport and chemical kinetics, a sensitivity analysis is performed for the three explosion limits at a fixed initial temperature of $T_0 = 760$ K. Figure 10 shows the most sensitive elementary reactions for each explosion limit. The sensitivity is expressed in terms of the change in the explosion pressure p_{Ex} resulting from a variation of the corresponding reaction rate coefficient: p^0_{Ex} refers to explosion pressure with unchanged rate coefficients, and p_{Ex} refers to explosion pressure after an increase in the rate coefficient of the reaction by a factor of two. The blue bars represent the reference case with the original molecular diffusion fluxes, whereas the red and yellow bars correspond to the cases in which the diffusion flux of H or H_2O_2 is reduced to 10% of its original value, respectively. The chemical sensitivities of the three explosion limits have already been extensively discussed in previous studies and are therefore not repeated here. Instead, the purpose of Fig. 10 is to examine whether modifying the diffusion fluxes changes the controlling chemistry and to quantitatively compare the influence of molecular transport with that of chemical kinetics. Overall, Fig. 10 shows that modifying species diffusion does not introduce a fundamentally different chemical mechanism. In other words, modifying either the H or H_2O_2 diffusion flux does not fundamentally change the reactions that control the corresponding explosion limits. More importantly, the magnitude of the transport-induced shift can be directly compared with the chemical sensitivities. At $T_0 = 760$ K, changing the H diffusion flux by a factor of two results in $\log_{10}(p_{Ex}/p^0_{Ex}) \approx 0.02$ at the first explosion limit. This effect is noticeably smaller than the sensitivities associated with the most important elementary reactions. Nevertheless, this should not be interpreted as indicating that an accurate description of H diffusion is unimportant. As discussed in Sec.4.2.2, H-radical transport has a pronounced influence on the subsequent flame propagation process. In contrast, changing the H_2O_2 diffusion flux by a factor of two at the third explosion limit results in $\log_{10}(p_{Ex}/p^0_{Ex}) \approx 0.12$. This magnitude is comparable to the sensitivities of the most influential elementary reactions shown in Figure 10. Therefore, under conditions near the third explosion limit, the

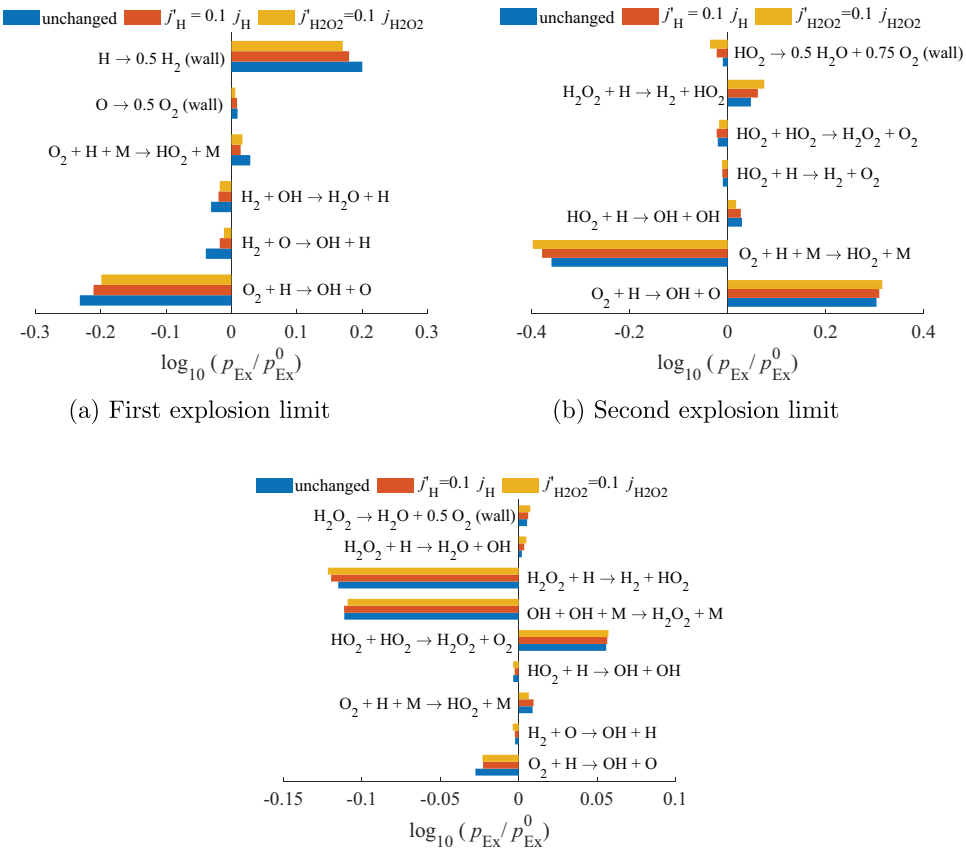

Figure 10. Sensitivity of the explosion pressure to the most influential elementary reactions at $T_0 = 760$ K for the first, second and third explosion limits. The blue bars represent the reference case with unchanged molecular diffusion fluxes, while the red and yellow bars correspond to reduced diffusion fluxes of H ($j'_H = 0.1j_H$) and H_2O_2 ($j'_{H_2O_2} = 0.1j_{H_2O_2}$), respectively.

influence of H_2O_2 molecular transport can be of similar importance to that of chemical kinetics. This quantitative comparison further shows that an accurate transport description is necessary for a physically consistent prediction of explosion limits.

Influence of molecular transport under lean and rich conditions

To understand whether the above conclusions regarding molecular transport are also applicable to non-stoichiometric mixtures, Fig. 11 compares the calculated explosion limits under lean ($\Phi = 0.4$) and rich ($\Phi = 4.0$) conditions using the same three transport models as in Figure 7. For both mixture conditions, neglecting thermal diffusion produces almost no change in the explosion limits compared with the detailed transport model, confirming that thermal diffusion remains negligible over the investigated range of equivalence ratios. This can be attributed to the fact, that in the initial phase, when the system "decides" ignition or not, the temperature gradients are still small. In contrast, the unity-*Le* assumption leads to noticeable deviations, particularly near the first and third explosion limits.

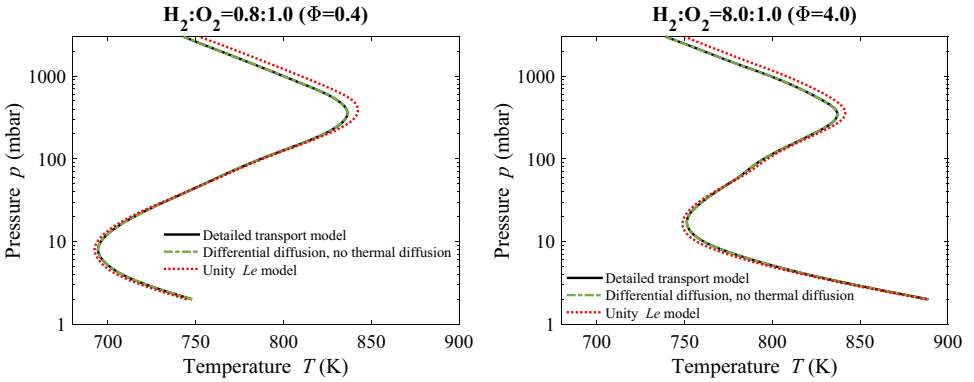

Figure 11. Calculated explosion limits for hydrogen-oxygen mixtures under lean condition ($\Phi = 0.4$, left sub-figure) and under rich condition ($\Phi = 4.0$, right sub-figure) with different transport models. Fixed temperature is used for temperature boundary condition.

These differences are consistent with the species-specific diffusion effects discussed above (c.f. Figure 7): H-radical diffusion is particularly important near the first explosion limit, whereas H_2O_2 diffusion becomes important near the third explosion limit. Since the underlying mechanisms have already been discussed in Secs.4.2.2 and 4.2.3, they are not repeated here. Overall, Fig. 11 suggests that the conclusions obtained for the stoichiometric mixture remain valid under both lean and rich conditions.

Implications for hydrogen safety

The results discussed in the present work have implications for hydrogen safety. The noticeable sensitivity of the third explosion limit to wall heat loss indicates that the thermal properties of the vessel and the associated heat-transfer conditions could significantly modify the conditions required for explosion. Hence, thermal management of wall material should be considered when assessing explosion risks in hydrogen-containing vessels. Furthermore, the strong influence of radical diffusion on explosion behavior suggests that controlling molecular transport may provide another possible strategy for explosion mitigation. For example, porous or radical-quenching materials could potentially modify radical transport and surface losses. Although such mitigation concepts are beyond the scope of the present study, the results show that energy and molecular transport are important physical factors that should be considered in future safety-oriented designs and modeling.

Conclusion

A detailed numerical investigation of explosion limits in hydrogen–oxygen mixtures has been performed using a one-dimensional spatially resolved model that consistently incorporates detailed chemistry, molecular transport, surface reactions and wall heat loss. The results confirm that the first and second explosion limits are predominantly chemically controlled and largely insensitive to wall heat loss, whereas the third limit is strongly

governed by the competition between heat release and heat dissipation at the wall, showing its fundamentally thermal character.

The potential influence of thermal diffusion (Soret effect) was also examined in the present simulations. Although the detailed results are not shown here, the calculations indicate that thermal diffusion has a negligible effect on the explosion limits under the considered conditions. This can be explained by the fact that ignition is initiated during a radical accumulation stage in which temperature gradients remain very small, and the corresponding thermal diffusion flux is therefore much weaker than the differential diffusion of radicals.

However, differential diffusion of key radicals plays distinct and physically important roles. Enhanced hydrogen radical H diffusion does not alter the explosion limits but significantly modifies the subsequent flame propagation speed after ignition. In contrast, enhanced H_2O_2 diffusion suppresses explosion near the third limit by weakening local chain-branching activity. These results show that molecular transport influences not only the onset of explosion but also the post-ignition flame evolution.

In contrast, homogeneous models, which neglect spatial temperature and concentration gradients and typically assume adiabatic conditions, cannot capture wall heat loss effects, radical redistribution, or flame propagation dynamics. While such simplified approaches may reproduce explosion limits, they fail to represent the underlying physical mechanisms governing different explosion regimes.

The present study therefore shows that accurate and physically reliable prediction of explosion limits requires the simultaneous consideration of energy transport and molecular diffusion. Spatially resolved modeling is essential to capture the intrinsic coupling between chemical kinetics and transport processes that controls both ignition and subsequent flame development.

Author contributions

CRediT: **Chunkan Yu:** Conceptualization, Formal analysis, Investigation, Methodology, Software, Validation, Visualization, Writing – original draft; **Liming Cai:** Formal analysis, Funding acquisition, Methodology, Writing – review & editing; **Ulrich Maas:** Conceptualization, Formal analysis, Funding acquisition, Investigation, Methodology, Software, Writing – review & editing.

Disclosure statement

No potential conflict of interest was reported by the author(s).

Funding

C. Yu and U. Maas acknowledge the funding by the Deutsche Forschungsgemeinschaft (DFG, German Research Foundation) under Research Unit [FOR5507] with project number [497007546]. The work from L.Cai was supported by the Science and Technology Commission of Shanghai Municipality [Grant No. 23160711900].

ORCID

Chunkan Yu http://orcid.org/0000-0002-0550-5003

References

Beeckmann J et al. 2017. Propagation speed and stability of spherically expanding hydrogen/air flames: experimental study and asymptotics. Proc Combust Inst. 360(1):0 1531–1538. https://doi.org/10.1016/j.proci.2016.06.194

Bird R, Stewart W, Lightfoot E. 2002. Transport phenomena. APPL MECH Rev. 55(1):R1–R4. https://doi.org/10.1115/1.1424298

Clark D, Simmons R, Smith D. 1970. Inhibition of the second limit of the hydrogen+ oxygen reaction by hydrogen bromide. Trans Faraday Soc. 66:0 1423–1435. https://doi.org/10.1039/tf9706601423

Giannakopoulos GK, Gatzoulis A, Frouzakis CE, Matalon M, Tomboulides AG. 2015. Consistent definitions of "flame displacement speed" and "markstein length" for premixed flame propagation. Combust Flame. 162(4):1249–1264. https://doi.org/10.1016/j.combustflame.2014.10.015

Heiple HR, Lewis B. 1941. The reaction between hydrogen and oxygen: kinetics of the third explosion limit. J Chem Phys. 9(8):0 584–590. ISSN 0021-9606. https://doi.org/10.1063/1.1750959

Hirschfelder JO, Curtiss CF, Bird RB, Mayer MG. 1964. Molecular theory of gases and liquids. New York: Wiley.

Kassel LS, Storch H. 1935. Chemical kinetics of the reaction of oxygen with hydrogen and with Deuterium1. J Am Chem Soc. 570(4):0 672–678.

Lee D, Hochgreb S. 1998. Hydrogen autoignition at pressures above the second explosion limit (0.6–4.0 MPa). Int J Chem Kinet. 300(6):0 385–406.

Lewis B, Von Elbe G. 2012. Combustion, flames and explosions of gases. Elsevier.

Li J, Liang W, Han W, Law CK. 2025. On explosion limits of hydrogen–oxygen mixtures with a catalytic platinum surface. Fuel. 391:0 134773. https://doi.org/10.1016/j.fuel.2025.134773

Liang W, Law CK. 2018. An analysis of the explosion limits of hydrogen/oxygen mixtures with nonlinear chain reactions. Phys Chem Chem Phys. 200(2):0 742–751.

Liu J, Wang J, Zhang N, Zhao H. 2018. On the explosion limit of syngas with CO2 and H2O additions. Int J Hydrogen Energy. 430(6):0 3317–3329. https://doi.org/10.1016/j.ijhydene.2017.12.176

Maas U, Warnatz J. 1988. Ignition processes in hydrogen- oxygen mixtures. Combust Flame. 740(1):0 53–69.

Maas U, Warnatz J. 1989. Ignition processes in carbon-monoxide-hydrogen-oxygen mixtures. In: Symposium (international) on combustion. Vol 22. Elsevier; pp 1695–1704.

Sánchez AL, Fernández-Tarrazo E, Williams FA. 2014. The chemistry involved in the third explosion limit of H2–O2 mixtures. Combust Flame. 1610(1):0 111–117. https://doi.org/10.1016/j.combustflame.2013.07.013

von Elbe G, Lewis B. 1942. Mechanism of the thermal reaction between hydrogen and oxygen. J Chem Phys. 100(6):0 366–393. ISSN 0021-9606.https://doi.org/10.1063/1.1723736

Wang X, Law CK. 2013. An analysis of the explosion limits of hydrogen-oxygen mixtures. J Chem Phys. 1380(13). https://doi.org/10.1063/1.4798459

Wang Z, Gou X, Zhang H. 2024. Explosion limit of hydrogen/oxygen mixture with water vapor addition. Int J Hydrogen Energy. 50:0 772–781. https://doi.org/10.1016/j.ijhydene.2023.06.321

Warnatz J, Maas U, Dibble RW, Warnatz J. 2006. Combustion. Springer.

Wen JX, Hecht ES, Mevel R. 2025. Recent advances in combustion science related to hydrogen safety. Prog Energy Combust Sci. 107:0 101202. ISSN 0360-1285. https://doi.org/10.1016/j.pecs.2024.101202

Williams FA. 2018. Combustion theory. CRC Press.

Zeldovich YB, Barenblatt G, Makhviladze G. 1985. The mathematical theory of combustion and explosions. Springer.